© 3rd IAHR Europe Congress, Book of Proceedings, 2014, Porto - Portugal. ISBN 978-989-96479-2-3

NUMERICAL SIMULATION OF THE FLOW AROUND A PIER USING OPENFOAM

PEDRO RAMOS, JOÃO PEDRO PÊGO & RODRIGO MAIA

Faculdade de Engenharia da Universidade do Porto, Porto, Portugal
pramos@fe.up.pt, jppego@fe.up.pt, rmaia@fe.up.pt

Abstract

Scour is a major source of damages to bridge foundations in riverbeds, which increases the risk of stability failure of the complete bridge structure. In Portugal, the tragic accident of *Entre-os-Rios* in the Douro river was partly due to scouring in one of the bridge piers.

Local scour around bridge piers has been investigated extensively. There are many studies about it, most of it based on experimental work, focusing on the prediction of maximum equilibrium depth. Nevertheless, there is still a lack of knowledge on the driving mechanisms that trigger and maintain the scouring process. The paper is intended to add knowledge to this field by means of numerical simulations.

The main goal of this study is the numerical simulation of the flow around an isolated circular pier, using the *OpenFOAM* toolbox, in two fixed bed configurations: one with a flat fixed bed, correspondent to the beginning of the scour process; the other representing the geometry of the bed after the equilibrium scour depth has been reached, that geometry being obtained experimentally. The velocity and vorticity field, the bed shear stress and the drag coefficient on the pier will be characterized for the two different configurations, applying the *Large Eddy Simulation* turbulence model.

The *OpenFOAM* results will be validated against data obtained with *Fluent* by Ramos (2012). *Fluent* and *OpenFOAM* are two CFD tools largely used in the industry and research on fluid mechanics, the first a proprietary software and the second a free and open source one. The two three-dimensional numerical models used allow to study flow structures like the horseshoe vortex, which has a crucial role in the scour process. The performance of both CFD tools will be analyzed and compared. The numerical results will be discussed and validated against data obtained from bibliography accepted as reference.

Keywords: Scour, *OpenFOAM*, Large Eddy Simulation, CFD.

1. Introduction and State of the Art

Local scour around bridge foundations can lead to the partial failure or the collapse of bridge piers. When a vertical circular pier is placed on the bed in a steady current it introduces changes to the flow pattern that interfere with the riverbed. Characteristic flow structures are the horseshoe vortex (formed in front of the pier) and the trailing vortex flow pattern (usually in the form of vortex shedding) that is formed at the lee-side of the pier (Figure 1). Also, there exists a downflow as a consequence of flow deceleration upstream of the pier. The overall effect of these changes is generally to increase the sediment transport, resulting in local scour around the pier.

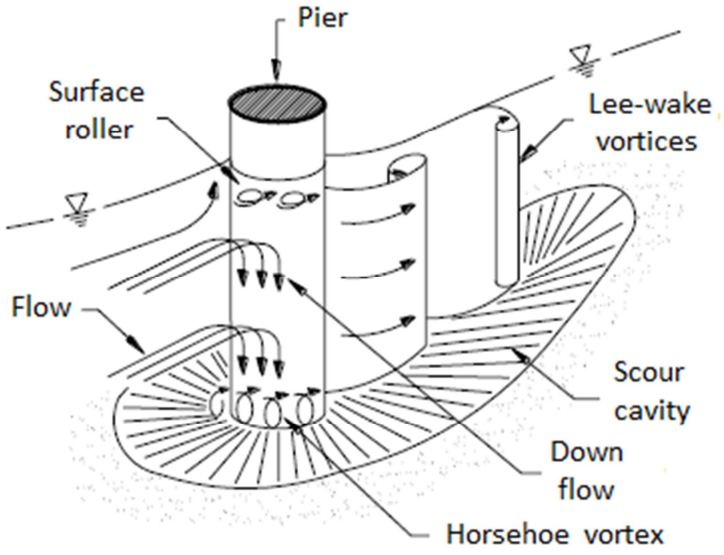

Figure 1. Flow around pier (reproduced from Breusers and Raudkivi, 1991).

Scour in piers is a complex phenomenon and, therefore, its study has been mostly experimental. Still, in the last years the first steps towards achieving the numerical simulation of this phenomenon have been taken.

Twaites (1960) and Bachelor (1967) reviewed the previous aerodynamic studies about the flow around cylindrical structures. Melville and Raudkivi (1977) presented the work that extended the aerodynamics studies to scour in piers, investigating the water-flow over a mobile sediment bed for different scour stages. A more detailed study was made by Melville (1988) and by Dargahi (1990).

Deng and Piquet (1992) developed a three-dimensional numerical simulation of the turbulent flow around an airfoil in which the main characteristics of the horseshoe vortex have been studied. That was one of the first works in CFD (*Computational Fluid Dynamics*) on this scientific field and it used a model based on the *Reynolds-averaged Navier-Stokes* (RANS) equations.

Richardson and Panchang (1998) simulated three-dimensionally the flow around a circular pier with a surrounding scour cavity to an intermediate phase and to the equilibrium phase. However, when comparing this study to the experimental data obtained by Melville and Raudkivi (1977) some discrepancies were found.

The works from Olsen and Melaaen (1993) is the first to combine flow simulation with scour modeling for a circular pier. Later, Roulund et al. (2005) performed the experimental and numerical simulation of flow and scour around the pier.

However, the turbulence model used was the *Shear Stress Transport* (SST) k-ω, which does an average of the length scales, not allowing, for example, to study of the wake vortices direct effect. In order to bridge this gap, Ramos (2012) simulated the flow around a circular pier using the LES model. The results of that work will be compared to ours.

2. Flow characteristics

The reference case used for this publication was the experimental and numerical work of Ramos (2012), developed on the Laboratory of Hydraulics of FEUP – Faculty of Engineering of University of Porto. The laboratory work was performed in a long water channel with 1 m width and 32.2 m length. In the bed of that channel was placed a PVC cylinder 0.05 m diameter (Figure 2). The bed material consisted of quartz sand with a median diameter (D_{50}) equal to 0.86 mm, with a coefficient of gradation (σ_D) equal to 1.5.

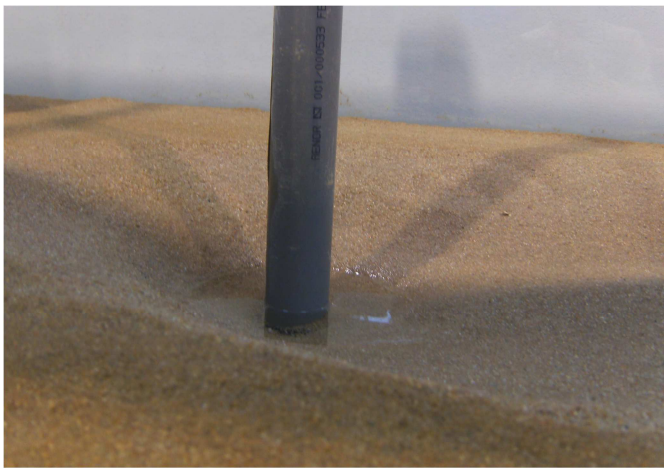

Figure 2. Scour cavity obtained in the laboratory test (Ramos, 2012).

The maximum depth of scour is obtained for flow conditions near to the critical speed ($U \approx U_c$), i.e., the mean flow velocity corresponds to the start of the particles motion (Melville and Coleman, 2000). Thus, the flow rate supplied was 64 l/s and the flow depth (h) equal to 0.20 m, resulting in a speed of 0.32 m/s. By the Shields diagram, the critical shear stress of the bed particles is 0.5 *Pa* (Ramos, 2012). This parameter will be useful to compare with the bed shear stress value obtained by *Fluent* and *OpenFOAM* simulations.

After 7 days, the maximum scour depth was 12.2 cm (Ramos, 2012). The geometry is represented by Figure 3, and it was simplified and transported to a 3D model to run the numerical simulations.

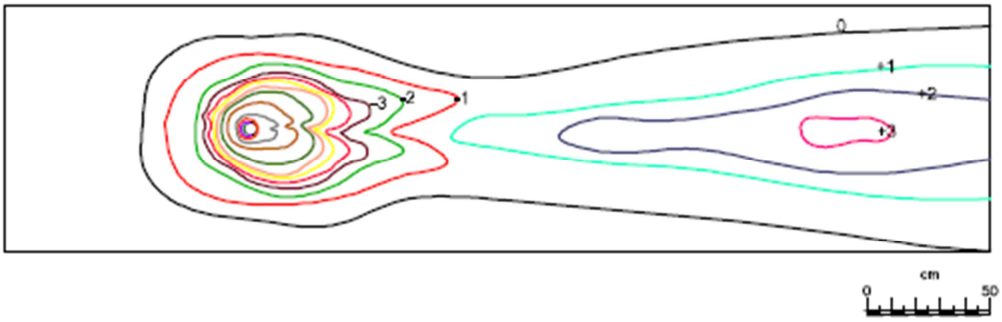

Figure 3. Final bed geometry (Ramos, 2012).

3. Numerical model

In the present study, the LES (*Large Eddy Simulation*) implementation was performed using the software *OpenFOAM*. A three-dimensional simulation is required because the goal is to examine the flow patterns around the pier and the role of the flow structures (vortexes) in the scour process.

The LES methodology assumes that smaller scales movements (small eddies/vortices) tend to be more homogeneous and isotropic, and thus less affected by the boundary conditions, unlike what happens with the larger scales (Figure 4). This makes simulation universal and constant in local conditions, what constitutes a major advantage over *Direct Numerical Simulation* (DNS), by solving the complete *Navier-Stokes* equations (Equation 1) only for the larger scales (the most energetic ones), leaving the smaller ones to be parameterized by incorporating a subgrid-scale model (Fergizer, 2002). The governing equations are shown in the Equation 1.

$$\frac{\partial}{\partial t}(\rho U_i) + \frac{\partial}{\partial x_j}(\rho U_i U_j) = -\frac{\partial p}{\partial x_i} + (\mu + \mu_T)\left(\frac{\partial U_i}{\partial x_j} + \frac{\partial U_j}{\partial x_i}\right) \quad [1]$$

Where U_i is the *i–th* component of velocity, t, the time, x_i, x_j, the Cartesian coordinates, ρ is the fluid density, p, the dynamic pressure, μ is the dynamic viscosity, and μT is the turbulent viscosity (Roulund et al., 2005).

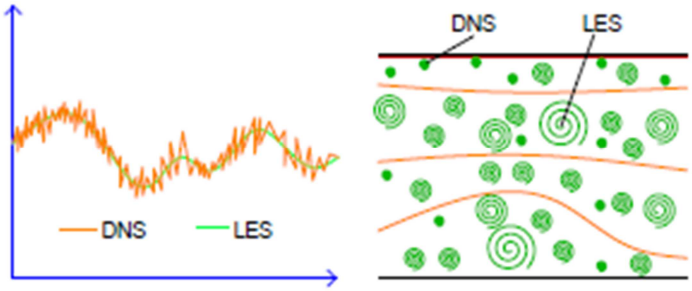

Figure 4. a) Velocity vs. time on a random point in a turbulent flow b) Different eddies sizes in turbulence (reproduced from Fergizer, 2002).

3.1 *OpenFOAM* case setting

In order to run the case with *OpenFOAM*, the first step was to build the mesh in the *blockMesh* utility. The most important improvement of this work, relatively to the previous one (Ramos, 2012), is the use of structured meshes (Figures 5 and 6). In both meshes, the zone around the pier is finer, as well as in the proximity of the walls and bed of the channel, but in the second one (Figure 5 - right and Figure 6) the cells are aligned and distributed in a regular way, which increases the velocity of data processing during the iterations.

However, the meshing process is complex, mainly if the goal is to adapt a regular mesh to a curve surface, like the cavity around the pier. So, contrarily to what was done in the work of Ramos (2012), the actual geometry of the scoured bed (Configuration B) was not accurately translated to a mesh. Instead of that, it has been simplified in order to have a regular distribution of the cells and thus a numerical problem less complex. This was an important step, since the LES model requires a lot of computation time.

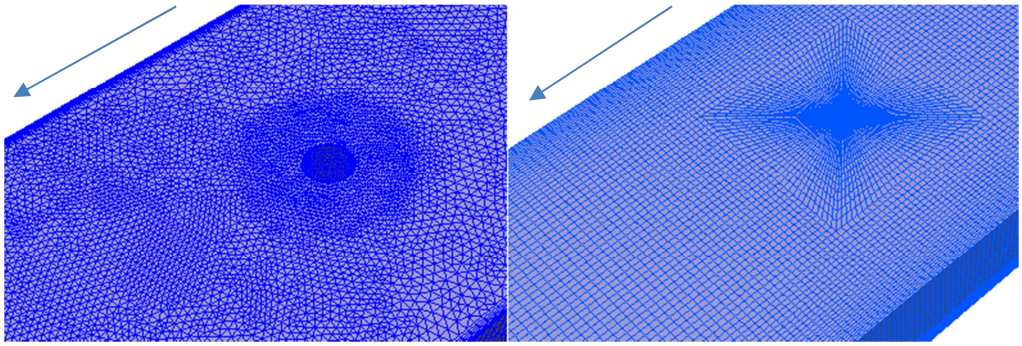

Figure 5. 3D representation of the meshes (left - Ramos (2012); right – *OpenFOAM*).

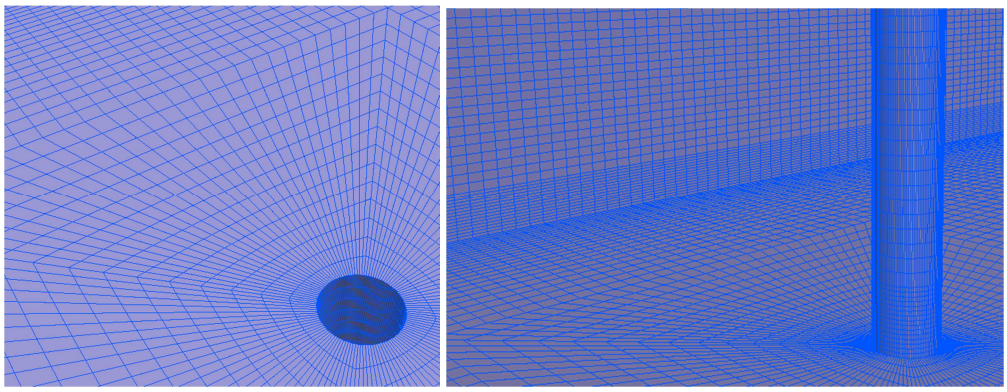

Figure 6. Details of the mesh used in *OpenFOAM* simulations.

The case requires initial and boundary conditions settings for all the involved fields (Figure 7). For applying boundary conditions, a boundary is broken up into a set of Patches. In this case the water enters perpendicularly to the inlet with a logarithmic profile (because of the *no slip* condition on the bed) with an average flow velocity of 0.32 m/s. The *OpenFOAM* solver used is *interFoam*, implemented for turbulent incompressible flow.

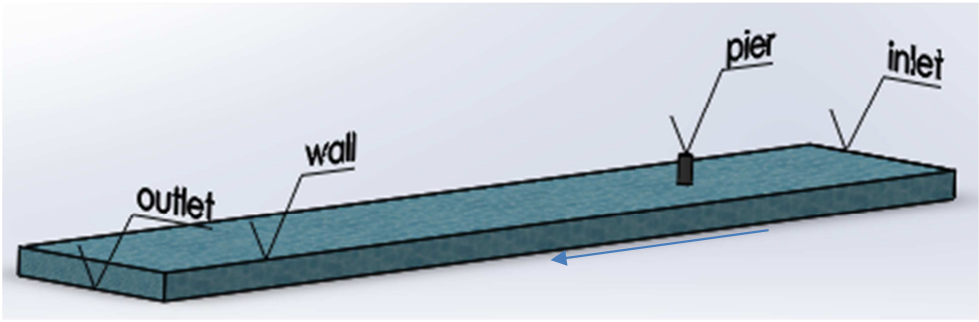

Figure 7. Schematic description of the geometry and its boundary-conditions.

4. Results analysis and comparison

The numerical data obtained by Ramos (2012) and in this work, with *OpenFOAM*, was visualized through an open source tool called *Paraview*. In the Figure 8 are represented the locations of the flow where it will be presented the numerical results. The plane 1 is parallel to the bed channel, on half depth of the flow. The plane 2 is the symmetry plane of the channel that contains the pier. Also, it will be presented the results for the shear stress on the bed channel and the drag coefficient on the pier.

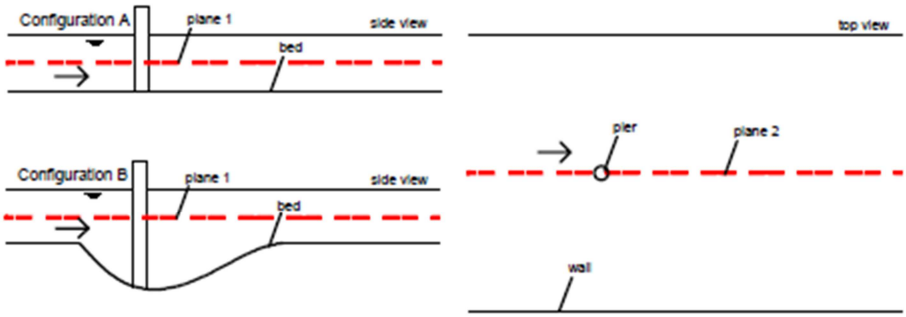

Figure 8. Schematic description of the configurations and the planes where are presented the velocity fields (left – side view; right – top view).

4.1 Configuration A (horizontal bed)

As stated earlier, the wake vortices play a very important role in the scour process, as they have the ability to unpin particles from the bed and transport them downstream. This spread can be seen in Figures 9 and 10 (*Fluent* and *OpenFOAM* results, respectively) through the contour of the instantaneous velocities in the horizontal plane at the mid-depth of the flow.

It should be noticed that as they move downstream, they lose intensity, which partly explains the fact that the scour depth is greater in the area closest to the pier, while downstream an accumulation of the particles is observed. In the simulation with *OpenFOAM* the wake vortex area is bigger and with more turbulence, closer to what it was observed in the laboratory. This is the first indicator that the improvement of the mesh leads to results with more consistency with the reality.

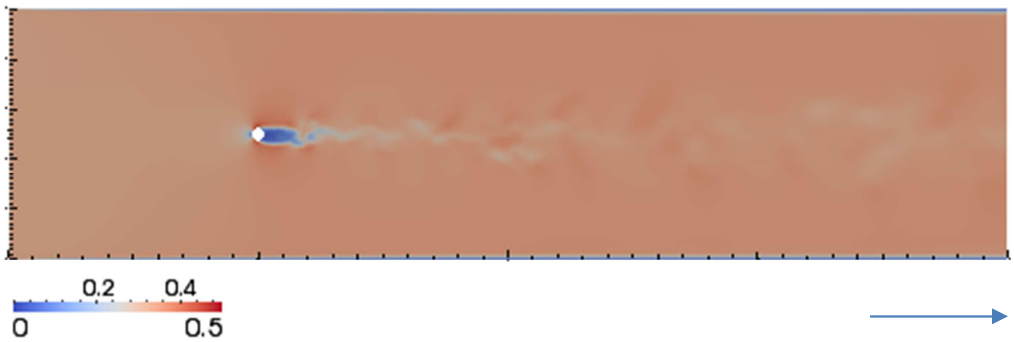

Figure 9. *Fluent* results to velocity field (m/s) (t=20s; Configuration A) in the parallel plane to the bed channel, on half depth of the flow (Ramos, 2012).

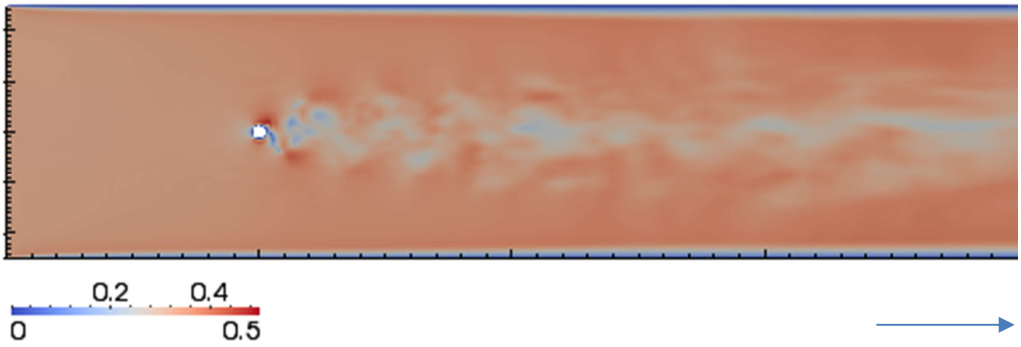

Figure 10. *OpenFOAM* results to velocity magnitude (m/s) (t=20s; Configuration A) in the parallel plane to the bed channel, on half depth of the flow.

In the work of Ramos (2012), only the water height (20 cm) was simulated. In the presented work it was simulated a two-phase flow, with an air layer (5 cm) and water layer (20 cm), by VOF (*Volume of Fluid*) method, what explains the different heights of the flow in the Figures 11 and 12). It was defined an initial velocity of the air equal to the velocity of the main flow (0.32 m/s).

Once again, it is clear a stronger turbulence in the second set of simulations. In Figure 12, the effect of the wake vortex shedding is more visible, like it happened with Figure 10. The turbulence coefficients in the both numerical model are the same, so this differences are due to the improvement the mesh and/or the application of the VOF method. In the *OpenFOAM* simulation (Figure 12) the velocity next to the bed channel, downstream the pier, is lower, showing that the suction effect of the bed particles due to the wake vortex shedding is stronger than in the previous simulation.

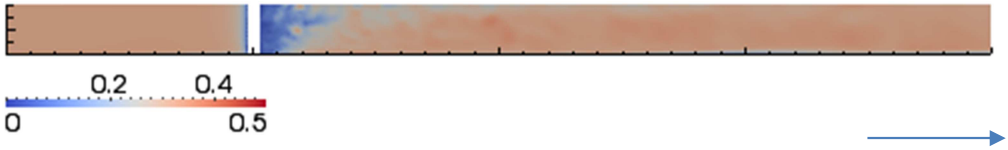

Figure 11. *Fluent* results to velocity magnitude (m/s) (t=20s**;** Configuration A) in the symmetry plane of the channel (Ramos, 2012).

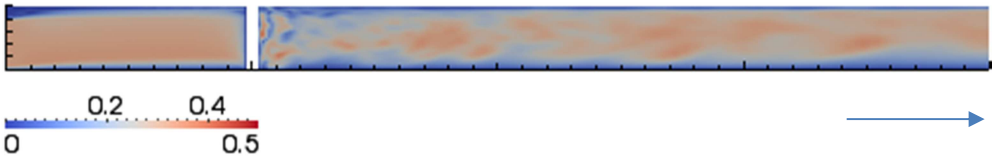

Figure 12. *OpenFOAM* results to velocity magnitude (m/s) (t=20s; Configuration A) in the symmetry plane of the channel.

The magnitude of the bed shear stress (Figures 13 and 14) is of the same order in both simulations, but its distribution around and downstream the pier has different shape in the two simulations. In Figure 14, the wake vortex effect on bed shear stress is more noticed.

The critical bed shear stress according to the Shields diagram is 0.5 *Pa*, so it is clear that the simulations shows that it will occur scour in the bed. In both simulations, the critical zone is on the sides of the pier. This shows that the scour process begins at these points, since this configuration represents an initial stage, before the scour process begins. From the authors' perspective, this can be an indicator that the scour process is initiate by the horseshoe vortex, since this vortexes spread by the side of the pier from upstream to downstream (Figure 1).

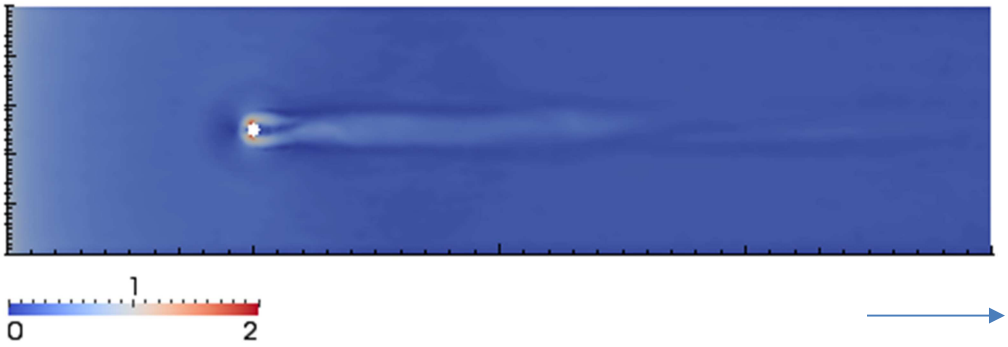

Figure 13. *Fluent* results to bed shear stress (*Pa*) (t=20s; Configuration A).

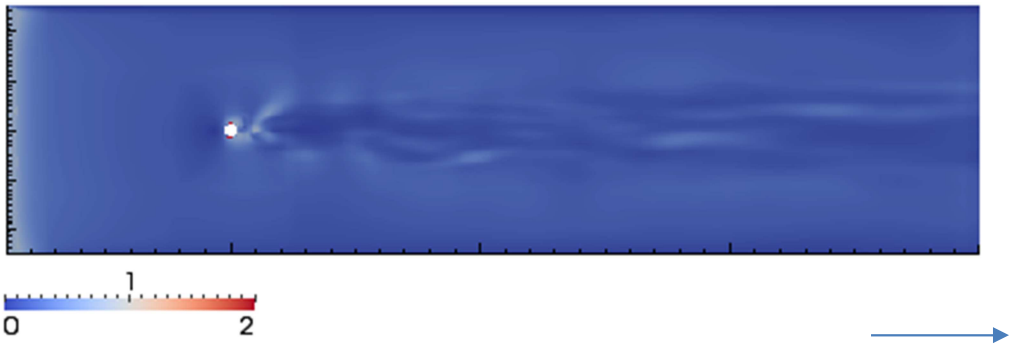

Figure 14. *OpenFOAM* results to bed shear stress (*Pa*) (t=20s; Configuration A).

In order to compute the drag coefficient, the *forceCoeffs functionObject* were used. The *functionObjects* are general libraries that can be attached run-time to any solver, without having to run again the simulation it is only needed calculate other additional parameter. So, the drag coefficient on the pier was calculated by the OpenFOAM toolbox based on the mentioned library, and recorded in function of the time flow simulated, with an average value of 1.21 (Figure 15), against the average value obtained in the *Fluent* simulations: 0.68 (Ramos, 2012). The range of time flow showed is short because of the instability of the solution in the first 10 seconds.

According to White (2006), by empirical formulas, the expected drag coefficient to this case is approximately 0.73. It is clear that the vortex shedding on the pier leads to oscillations of the drag force on the pier. The smaller oscillations are due to the turbulent nature of the flow. The frequency of these oscillations is a relevant information to the dynamic analysis of the structure which the pier belongs. The drag coefficient behavior through time is similar to the described by Jongho *et al*. (2011).

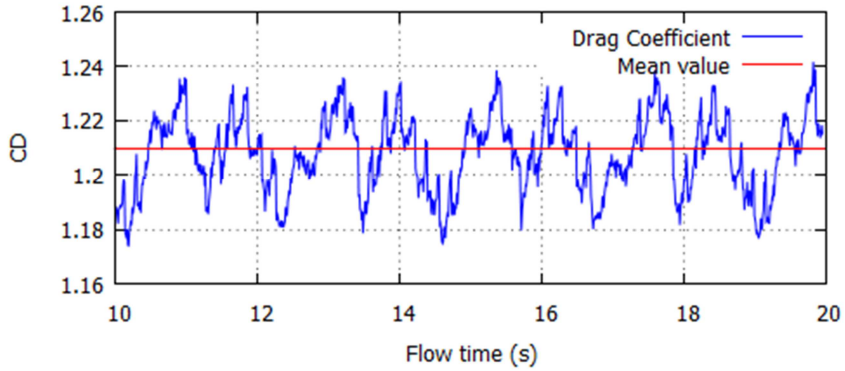

Figure 15. Drag coefficient vs. flow time (Configuration A).

4.2 Configuration B (scoured bed)

Once again, the wake vortex is less visible in the *Fluent* simulation. However, it seems that these vortexes lose intensity faster than in the Configuration A due to the new bed topology (Figures 16 and 17). This is plausible, because if the wake vortex showed the same intensity, there will be scour, which would not be coherent with this configuration, since it represents the equilibrium scour depth situation.

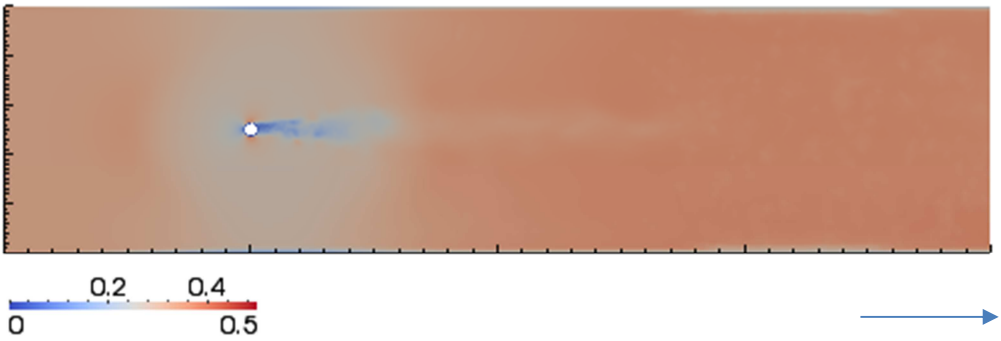

Figure 16. *Fluent* results to velocity magnitude (m/s) (t=20s; Configuration B) in the parallel plane to the bed channel, on half depth of the flow (Ramos, 2012).

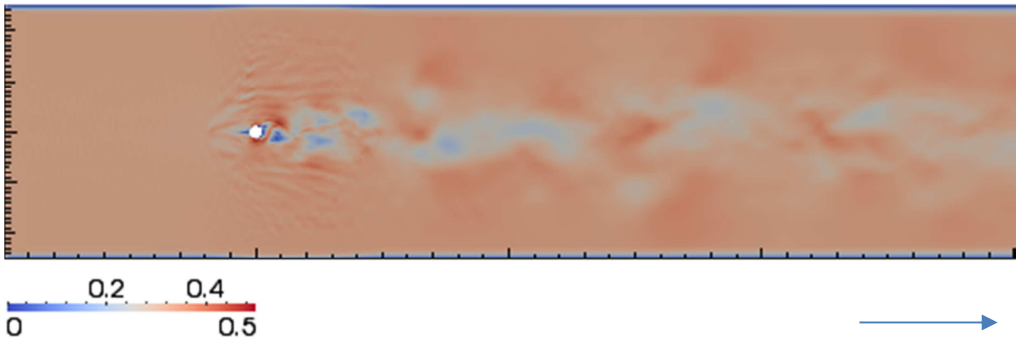

Figure 17 - *OpenFOAM* results to velocity magnitude (m/s) (t=20s; Configuration B) in the parallel plane to the bed channel, on half depth of the flow.

In Figure 18, upstream the pier, it is visible a small area, with very low velocity magnitude, that may correspond to the horseshoe vortex, according to Ramos (2012). The horseshoe vortex is a small and complex vortex system and it is not easy to compute. In the *OpenFOAM* simulation it is not clear this phenomenon, but in the correspondent zone there is much turbulence (Figure 19), which is a good signal.

In Configuration B, lower bed shear stress values are expected, all of them above the critical bed shear stress (0.5 *Pa*). It is harder to compute this parameter, relatively to the previous configuration, due to the more complex bed geometry. However, both simulations show values that match with an equilibrium scour depth situation.

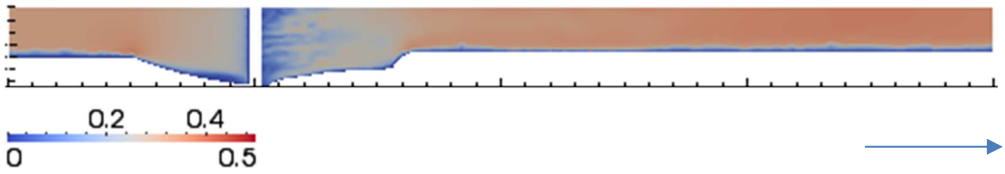

Figure 18. *Fluent* results to velocity magnitude (m/s) (t=20s; Configuration B) in the symmetry plane of the channel (Ramos, 2012).

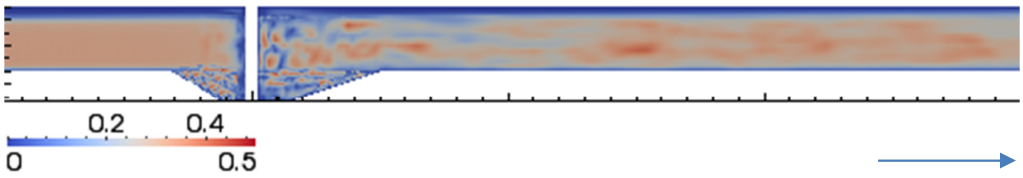

Figure 19. *Fluent* results to longitudinal velocity (m/s) (t=20s; Configuration B) in the symmetry plane of the channel (Ramos, 2012).

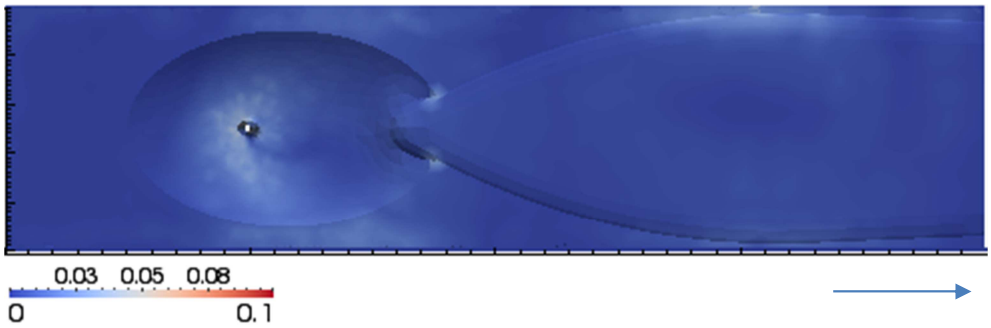

Figure 20. Fluent results to bed shear stress (*Pa*) (t=20s; Configuration B).

The evolution of the drag coefficient in time is more irregular in this configuration, and with a bigger amplitude of values. The average value (0.053) is smaller than the previous configuration (1.21) and bigger than the average value given by *Fluent* simulation (0.41) (Ramos, 2012).

Figure 21. *OpenFOAM* results to bed shear stress (*Pa*) (t=20s; Configuration B).

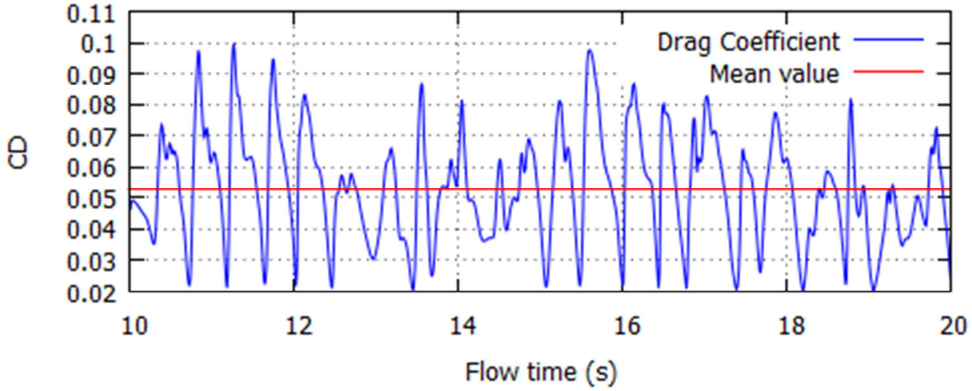

Figure 22. Drag coefficient vs. flow time (Configuration B).

5. Conclusions

The three-dimensional numerical simulation of the flow around a pier has been developed using *OpenFOAM* toolbox. The turbulent flow was simulated for a flat bed situation and for a configuration with a scoured bed, using the Large Eddy Simulation turbulence model. Some of the results were compared with the simulations of the same flow, obtained by Ramos (2012) with the commercial software *Fluent*.

To the Configuration A (flat bed situation), it was used a regular mesh, contrarily to what was done in the work of Ramos (2012), a fact that clearly improved the quality of the results. To the second configuration (equilibrium scour depth situation), it was applied again a regular mesh, and for that, a simplification of the irregular bed has to be done, preventing problems due to the complex geometry of the bed sand. The computation of the vortexes improved, mainly of the wake vortex shedding. The appearance of the horseshoe vortex in the velocity fields is not clear, despite the perturbation observed in the scour cavity, immediately upstream the pier.

From the authors' point of view, the simulations obtained by each software (*Fluent* and *OpenFOAM*) present a reasonable qualitative and quantitative concordance between them, and with the expectable from what was observed in the laboratorial test executed by Ramos (2012). The results for the drag coefficient on the pier matche with the values given by empirical formulas (White, 2006).

However, there is much space for improvements. *OpenFOAM* has all the advantages offered by a free and open source software. Unfortunately, the lack of a graphical user interface makes the pre-processing a difficult task. However, it has been shown that *OpenFOAM* may be suitable for running CFD simulations in place of a commercial code like *Fluent*.

Although the residuals of the iterations of the both simulations pointed to the convergence of the solution, in a work of this kind, perfect results cannot be expected, due to the large number of factors involved which cannot be simulated directly using a numerical model. However, the overall picture is quite positive, mainly because of the improvement in the quality of results, comparably to the last work of Ramos (2012).

Acknowledgments

This publication is supported by the European Regional Development Fund (FEDER) through the funds of the Competitiveness Factors Operational Programme (COMPETE) and with national funds from the Portuguese Foundation for Science and Technology (FCT) under the project "Numerical and experimental study of the flow around complex bridge piers" (Ref. FCT EXPL/ECM-HID/1663/2013).

References

Batchelor, G. K. (1967) *An introduction to fluid dynamics*. University Press, Cambridge.

Breusers, H.; Raudkivi, A. J. (1991) *Scouring*. IAHR Hydraulic Structures Design Manual. A. A. Balkema, Rotterdam, Netherlands.

Dargahi, B. (1990) *Controlling Mechanism of Local Scouring*, J. Hydr. Engrg, ASCE, Vol 116, No.10

Deng, G.; Piquet, J. (1992) *Navier-Stokes computations of horseshoe vortex flows*. Int. J. Numer. Meth. Fluids, 15: 99–124.

Ferziger, J.H.; Peric, M. (2002) *Computational Methods for Fluid Dynamics*. Springer, Berlim.

Jongho L., Jungwoo K., Haecheon C. (2011) *Sources of spurious force oscillations from an immersed boundary method for moving-body problems*, Journal of Computational Physics, Vol. 230, Issue 7.

Melville, B.; Coleman S. (2000) *Bridge Scour*; Water Resources Publications LLC, (2000) Colorado, U.S.A.

Melville, B.; Raudkivi, A.J. (1977) *Flow characteristics in Local Scour at Bridge Piers*, J. Hydr. Research, ASCE, Vol 15, pp. 373-380.

Olsen, N.R.B.; Melaaen, M.C. (1993) *Three-dimensional calculation of scour around cylinders*. Journal of Hydraulic Engineering (ASCE), 119, 1048–1054.

Ramos, P.X. (2012, *Modelação numérica do escoamento em torno de um pilar*, MSc Thesis at Faculty of Engineering of University of Porto, Portugal.

Richardson, J.; Panchang, V. (1998) *Three-dimensional simulation of scour-inducing flow at bridge piers*. Journal of Hydraulic Engineering.

Roulund, A.; Sumer, M. Fredsøe, J. Michelsen, J. (2005) *Numerical and experimental investigation of flow and scour around a circular pile*. Journal of Fluid Mechanics, 534, pp 351- 401.

Thwaites, B. (1960) *Incompressible aerodynamics*. University Press, Oxford.

White, F. (2006) *Fluid Mechanics*. McGraw-Hill Companies; 6th edition.